

Thermal-Mechanical Characterization of Polyurethane Rigid Foams: Effect of Modifying Bio-Polyol Content in Isocyanate Prepolymers

Luis Daniel Mora-Murillo¹, Felipe Orozco-Gutierrez², José Vega-Baudrit² and Rodolfo Jesús González-Paz^{2*}

¹*School of Chemical Engineering, University of Costa Rica, San Pedro Montes de Oca, San José, Costa Rica*

²*National Nanotechnology Laboratory, National Center for High Technology, San José, Costa Rica*

Received November 25, 2016; Accepted February 14, 2017

ABSTRACT: Nowadays, green polyurethane (PU) foams are mostly synthesized by replacing an amount of petrochemical polyol with biobased polyol. Here we report five different families of isocyanate prepolymer formulations that were prepared with biobased sources and the correlation between the structure of chains and the properties of the produced PU foam. Foam behavior in tension, torsion, compression, shape memory tests and physical properties were studied by dynamic mechanical thermal analysis (DMTA); interactions in the polymer chains were analyzed by Fourier transform infrared spectroscopy (FTIR); and thermal analysis was performed by thermogravimetry (TGA) and differential scanning calorimetry (DSC). The results showed that high content of biobased macrotriol in the prepolymer formulation implies a softer final material than commercial polyester polyol foams due to the branched biobased molecules that do not allow enough packaging of the polymer matrix. Moreover, mechanical and thermal properties of the final PU foam are affected by the length, functionality and polarity of the biobased molecules used in the isocyanate prepolymer synthesis.

KEYWORDS: Biobased polyurethane, prepolymer, biodegradable, renewable resources, thermal-mechanical properties

1 INTRODUCTION

Polyurethane (PU) foams are usually obtained by mixing two parts: an isocyanate prepolymer and a polyol mixture of organic molecules containing at least two hydroxyl groups obtained from petroleum. The PU prepolymers consist of a macromolecular chain mixture with many urethane groups in its backbone and an isocyanate reactive group at the chain's end, which allows one to control the viscosity, reactivity and toxicity of the PU component [1]. Secondary reactions can take place when foaming. The reaction between water (blowing agent) and isocyanate groups generates amines and gaseous CO₂, helping the foam growth; these produced amines can also react with the isocyanate to form ureas and isocyanate that can react with themselves in a trimerization reaction to form isocyanurates [2].

Estimated at nearly two billion kilograms in the US alone, PU foams currently account for the largest market among polymeric foams [3]. The versatile

properties offered by this material are suitable for use in many fields such as medical devices, coatings and paints, elastic fibers, rigid insulations or flexible and rigid foams. Since petroleum is a nonrenewable source, in recent years there has been increased interest in the synthesis of polymers starting from renewable raw materials, like vegetable oils and natural fats, because of their relevant properties such as availability, low toxicity, sustainability and biodegradability [4, 5].

Considering all of these facts, it is necessary to find alternative routes using natural resources that can help to reduce greenhouse effect emissions in comparison with the fabrication process of conventional polyurethane foams that use raw materials derived from petroleum. The fact that PU foams obtained from natural resources may have biodegradable properties should not be ignored, so the material will also degrade in a more environmentally friendly way [5]. Many studies focused on the synthesis of biobased polymers have tested and reported that vegetable oils are good precursors of polyurethane materials [6–8].

Vegetable oils can be used directly as monomers as found in nature or can be modified with chemicals or

*Corresponding author: rgonzalez@cenat.ac.cr

enzymes to obtain a specific structure [9]. Vegetable oils are triglycerides (esters of glycerol with three long-chain fatty acids) [10]. The structure of triglycerides depends on the source of the oil; this means that each fatty acid could have many double bonds and different strategic reactive moieties such as hydroxyl groups on the hydrophobic backbone [10].

Products such as ethylene glycol, ethylene dichloride, styrene ethylbenzene, chloroethanol, vinyl chloride, and vinyl acetate come from the petrochemical industry [11]. Many other substances can also be synthesized by raw material polymerization to produce a variety of organic chemical products such as polyethylene, polyvinyl chloride, and polystyrene [11]; for this reason, recent efforts to find alternative ways to substitute traditional hydrocarbon cracking have increased. Such innovative ways to produce monomers would reduce greenhouse gas emissions and dependency on limited fossil fuels; for example, it is now possible to obtain monomers from renewable resources such as ethylene glycol from ethanol by a catalytic dehydration [12] or the synthesis of ethylene glycol from cellulose over Ni-WO₃/SBA-15 catalysts [13, 14].

In this study, biobased PU rigid foams were synthesized using polyols from renewable resources to investigate the effects of the structure on various properties, including the thermal-mechanical behavior according to the content of polyols in the isocyanate prepolymer. As a result, families with short chain diol content in the prepolymer create more physical cross-linking with other chains due to the higher frequency of urethane groups in polymer chains. The shape fixity values obtained for PU 3 and PU 4 were 88.5 and 85.8, respectively.

2 EXPERIMENTAL SECTION

2.1 Materials

The biobased polyols and toluene diisocyanate (TDI) for the prepolymer preparation were purchased from

the Costa Rican market by GOVAN PROJECTS S.A. Characteristic properties such as viscosity and %NCO (% g NCO/g sample) of isocyanate prepolymers were measured according to ASTM standard D2572 - 97 [15]. Also, acid value and OH number of the polyols used to synthesize the prepolymers were confirmed based on ASTM standards D1980 - 87 [16] and D4274 -11 [17], respectively. Short chain bio-diol (molecular weight = 62 g/mol and hydroxyl value of 1808 mg KOH/g), bio-macrodial (average molecular weight = 400 g/mol and hydroxyl value of 281 mg KOH/g) and bio-macrotriol (molecular weight = 933 g/mol and hydroxyl value of 163 mg KOH/g) were dried with a rotary evaporator in an attempt to reduce the water content as much as possible to avoid secondary reactions during the prepolymer synthesis. For foam synthesis, a commercial petroleum-derivate polyol was used (with a hydroxyl value of 565 mg KOH/g and an acid value of 1,57 mg KOH/g), donated by GOVAN PROJECTS S.A. Other reagents such as hydrochloric acid (HCl), isopropyl alcohol, pyridine, acetic acid, acetone and toluene were used as received from the local market.

2.2 Synthesis of Biobased Isocyanate Prepolymer

As a first step, it was necessary to dry all bio-polyols at 80 °C and 40 Pa for 2 hours in a rotary evaporator to avoid the presence of water during the prepolymer synthesis. Once the bio-polyols had no moisture, the prepolymers were synthesized by reacting difunctional or tri-functional polyols (Table 1) and an excess of diisocyanate. The synthesis was carried out in a 250 mL Erlenmeyer flask including a magnetic stirrer and nitrogen gas inlet.

Polyols were added to the reactive system and mixed with a magnetic stirrer at 375 RPM; when the mix of polyols reached 60 °C, TDI was charged in the container and the reaction started for two hours.

Table 1 Formulation and properties for synthesized biobased isocyanate prepolymers.

Sample	Distribution of OH molar fraction contributed by bio-polyols in the prepolymer (%)			%NCO	Viscosity (mPa·s)
	Short chain diol	Macrodial	Macrotriol		
PUP 1	0	65	35	33.5	509.9
PUP 2	0	35	65	32.3	287.9
PUP 3	11	24	65	32.3	435.5
PUP 4	17.5	17.5	65	32.1	513.6
PUP 5	0	0	100	33.0	250.7
PUP REF	–	–	–	30.8	3000.0

2.3 Biobased Polyurethane Foaming

Initially a commercial petro-based polyol was added into a 25 mL beaker, and then the biobased isocyanate prepolymer was added into the container. The quantity of each component changed depending on the NCO percentage of the prepolymer, but always keeping the NCO/OH ratio of 1.5. All materials were thoroughly mixed with an IKA T25 digital Ultra Turrax at 4000 RPM for 1 minute. Subsequently, 18 g of the total formulation was poured into a closed mold at 44 °C (regulated by a water recirculation system). Foams were in the mold for 45 min and then they were cured at ambient conditions for a week before characterization. Foams with standard commercial densities are around $50 \pm 10 \text{ kg/m}^3$. Once the curing period was finished, the foam was cut into different sizes with a scalpel in order to proceed with the corresponding characterization.

2.4 Characterization

2.4.1 Fourier Transform Infrared Spectroscopy (FTIR)

The FTIR spectrums were performed using a Thermo Scientific Nicolet 6700 spectrometer within the frequency range of 4000–600 cm^{-1} in attenuated total reflection infrared (ATR) mode. A resolution of 4 cm^{-1} was used.

2.4.2 Mechanical Properties Tests

Mechanical properties of the foams were tested on a DHR III rheometer from TA Instruments to measure the stress-strain behavior of the samples on tension, torsion and compression modes.

For tension tests, samples of $40 \times 5 \times 3$ (mm \times mm \times mm) were stretched with a ratio of 0.6 mm/min, and axial force vs. displacement values were registered according to ASTM D1623-09. In compression tests the size of specimens was $10 \times 10 \times 10$ (mm \times mm \times mm), the strain rate was fixed at 3 mm/min and axial force vs. displacement values were recorded until 10% strain parallel to foam rising according to ASTM D1621-10. Finally, for torsion tests, the sample size used was $50 \times 10 \times 5$ (mm \times mm \times mm) and a shear rate of $1.59092 \times 10^{-3} \text{ s}^{-1}$ was applied during 300 s. Stress vs. strain data was saved for torsion essays. All mechanical tests were realized under ambient conditions.

2.4.2 Differential Scanning Calorimetry (DSC)

The DSC curves were obtained in a Q200 differential scanning calorimeter from TA Instruments. Samples of

~ 2.5 mg were encapsulated in an aluminum pan and heated at a rate of 10 °C/min from -60 to 250 °C under a nitrogen atmosphere to determine the glass transition temperature (T_g) and the curing temperature (T_c).

2.4.4 Thermogravimetric Analysis (TGA)

The thermal analysis of PU foams was performed on a TA Instruments Q500 thermogravimetric analyzer. Samples of ~ 5 mg were heated from 30 °C to 700 °C at a heating rate of 10 °C/min; then a 20 °C/min ramp was used from 700 °C to 1000 °C. All the experiments were done under nitrogen atmosphere.

2.4.3 Dynamic Mechanical Thermal Analysis (DMTA)

Dynamic mechanical thermal measurements were carried out on a DHR III rheometer from TA Instruments, applying an oscillatory stress to PU foams. In this case, stresses that cause 0.2% of strain in torsion mode are used with a 3 °C/min ramp temperature from 25 °C to 250 °C; the angular frequency was fixed at 2 Hz. $\tan \delta$ and G' values were registered.

2.4.6 Shape Memory Test

Shape memory tests were performed on a TA Instruments DHR III rheometer. To quantify the shape memory behavior, tests were performed in torsion mode, using a specimen size of $50 \times 10 \times 5$ (mm \times mm \times mm). The sample was first heated up to a temperature of $T_{\tan\delta} + 20$ °C; once the sample was stabilized, it was deformed from 0 kPa to 3 kPa torsion stress during a time interval of 100 s. After that, the sample was cooled to $T_{\tan\delta} - 20$ °C at a rate of 40 °C/min, and as the third step of the cycle, the strain was released from 3 kPa to 0 kPa during another interval time of 100 s (unloading). Finally, the sample was heated back up to $T_{\tan\delta} + 20$ °C at a rate of 5 °C/min, maintaining 0 kPa of torsion stress.

Rate of shape fixity, R_f , and rate of shape recovery, R_r , values for all samples were calculated according to the following equations:

$$R_f = \frac{\varepsilon_u}{\varepsilon_m} \times 100 \quad (1)$$

$$R_r = \frac{\varepsilon_m - \varepsilon_p}{\varepsilon_m} \times 100 \quad (2)$$

where ε_m represents the strain of the sample after the initial stress is applied at $T_{\tan\delta} + 20$ °C, ε_u is the strain after the strain had been released and the temperature had been held and ε_p is the strain measured after the heating in the final step of the cycle [18].



2.4.7 Density

The density of PU foam specimens was measured according to ASTM D1622-03. The sample size for density test was $110 \times 30 \times 30$ (mm \times mm \times mm).

3 RESULTS AND DISCUSSION

Table 1 shows the formulations used for the prepolymer synthesis.

3.1 Fourier Transform Infrared Spectroscopy (FTIR)

Differences in the structure given by the polyols used for the biobased isocyanate prepolymers synthesis was analyzed by FTIR spectra. Figure 1 shows the spectra of PU foams using the prepolymers specified in Table 1. As part of the main peaks, a signal around ~ 3310 cm^{-1} can be observed, which is attributed to the N-H stretching vibration [19]; but this region also presents a little shoulder at 3500 cm^{-1} in all the curves that corresponds to the non-H-bonded N-H group [20]. When the ~ 3500 cm^{-1} peak is present, it indicates that urethane and urea groups are not interacting with other chains of the polymers formed and the intensity of the ~ 3310 cm^{-1} band decreases, indicating a significant decrease in the intermolecular interaction. On the other hand, when N-H groups are interacting with hydrogen bonds with other polymer chains, the ~ 3500 cm^{-1} signal decreases [1]. In Figure 1 it can be observed that PU 5, which contains 100% of macrotriol in the prepolymer, presents fewer interactions by hydrogen bonds compared with N-H and PU 1 because of the steric hindrance produced by the branched (triol) and

large size of the molecule, which blocks the interactions between chains [1].

In Figure 1a, signals around ~ 2900 cm^{-1} are assigned to CH groups, specifically ~ 2920 cm^{-1} corresponding to asymmetric CH_2 stretching and 2860 cm^{-1} peak associated with symmetric CH_2 stretching. Asymmetric CH_3 stretching peak (2965 cm^{-1}) only appears clearly for the commercial PU foam [21] and PU 5 FTIR spectra that shows a small shoulder; this peak can be viewed only for this foam due to the higher concentration of CH_3 groups compared with the other formulations. All these signals are assigned to the flexible segments of the PU matrix [19], so PU formulations with more macrodiol and macrotriol present signals with more intensity in this zone.

Then, two signals at 1707 and 1600 cm^{-1} indicate the existence of C=O interacting with H bound urethane and C=C aromatic stretching vibrations, respectively [19,22]. These peaks are directly related to the hard segments of the polyurethane chains, which happens because the aromatic rings of the TDI give rigidity to chains. So, increasing short chain diol content in the prepolymer would produce higher frequency of aromatic rings and urethane groups in polymer chains, which are able to interact with other chains to form H bonds and, because of that, foams become more rigid [23].

The peak at ~ 1528 cm^{-1} is attributed to the N-H bending and to the urethane group and C-C/C-N stretching. So, this signal can be associated with the reactivity of each bio-polyol due to molecule size or steric hindrance. In this zone, PU 2 has the more intensive peak that is associated with the formation of more urethane bonds, and also the presence of high content of C-C groups in the macrotriol molecule. Short

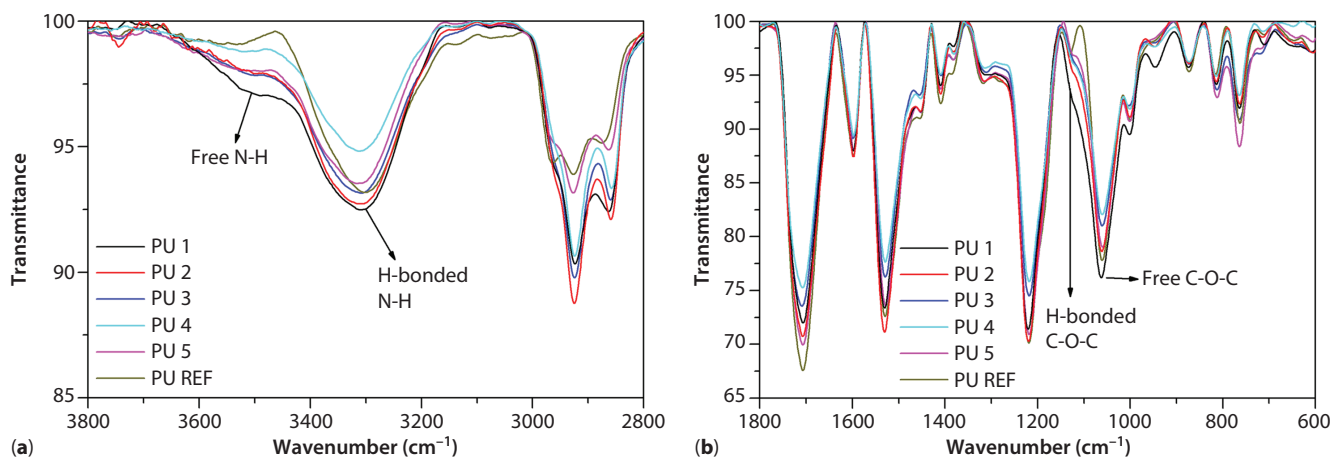


Figure 1 FTIR spectrum of biobased PU foams: (a) Section of FTIR spectrum at high wavenumbers and (b) Section of FTIR spectrum at low wavenumbers.

chain diol and macrodiol have more content of C=C compared to the macrotriol [24]. Peaks at $\sim 1450 \text{ cm}^{-1}$ can be related to CH_3 and CH_2 . The $\sim 1061 \text{ cm}^{-1}$ signal corresponds to C-O-C stretching vibrations [9]; this is a characteristic band of the urethane group. PU REF, which is the sample with less interactions in the N-H bound groups by hydrogen bonds, presents a peak at 1127 cm^{-1} related to hydrogen bound C-O-C groups; this means that decreasing the peak at 3500 cm^{-1} could result in the appearance of another signal at 1127 cm^{-1} . Other signals are identified in Table 2.

3.2 Mechanical Properties of Foams

Once PU foams have been cured for a week, mechanical properties are measured with the rheometer to analyze the dependence of mechanical behavior on the structure of the chains synthesized during the

Table 2 Interpretation of principal FTIR peaks obtained for PU molded foams.

Peak position (cm^{-1})	Characteristic absorption bands
3500	ν Free N-H stretching
3310	ν Bound N-H stretching
2965	νCH_3 stretching
2920, 2860	νCH_2 stretching
2270	Isocyanate group
1707	C=O stretching vibrations interacting with H bound urethane
1600	C=C aromatic stretching vibrations
1528	$\delta\text{N-H} + \nu\text{C-N} + \nu\text{C-C}$
1450	CH_2 scissoring and CH_3 deformation
1220	C-N bending
1127	Free C-O-C stretching (urethane, urea)
1060	H bound C-O-C stretching (urethane, urea)

prepolymer preparation; and due to the content of short, long or branched polyol, the soft or hard segments produced in the polymer network, the flexibility of the polyol molecules and the interactions between chains. Figure 2 shows the stress-strain curves in torsion mode for the PU samples of Table 1 and elastic modulus was calculated and reported in Table 3.

As can be appreciated, PU REF has the better behavior when a torsion stress is applied, and the curve is just above the PU 3 curve. This is explained by the balance obtained between the high content of macrodiol and the high molecular weight of macrotriol in the sample; the short diol is able to create hydrogen bonds in the polymer network and the well-distributed macrotriol in PU 3 formula generates a good crosslinked foam, resulting in good mechanical properties [1]. On the other hand, PU 5 presents bad mechanical behavior because of the absence of short or macro diol; as a result, this foam would present a very high content of soft segments in the chains.

Tensile behavior of bio PU foams is shown in Figure 3. In this figure, it can again be appreciated that

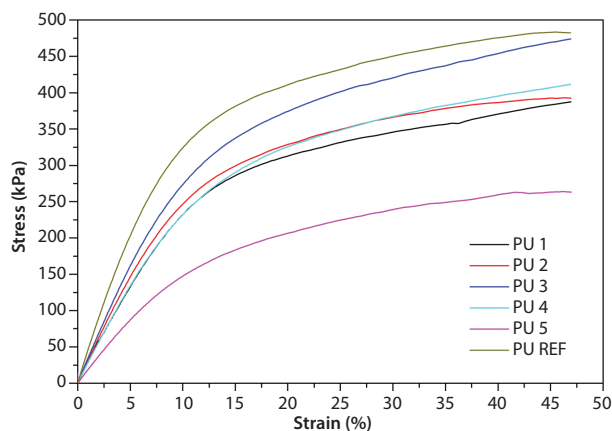


Figure 2 Stress-strain curves for biobased PU foams in torsion mode.

Table 3 Mechanical and thermal properties of biobased PU foams.

Sample	Density (kg/m^3)	E_{com}^a (MPa)	E_{tens}^a (MPa)	E_{tor}^a (MPa) ^{b c}	T_g^b ($^{\circ}\text{C}$)	T ($^{\circ}\text{C}$)	$T_{10\%}^c$ ($^{\circ}\text{C}$)	$T_{\text{tan}\delta}^a$ ($^{\circ}\text{C}$)
PU 1	51	4.46	4.50	2.33	7.65	67.50	251.5	127
PU 2	65	4.39	4.70	2.48	7.17	67.04	253.5	130
PU 3	52	4.00	4.48	2.75	6.69	63.12	252.2	143
PU 4	50	5.58	4.48	2.33	9.60	65.87	253.3	135
PU 5	69	2.71	3.58	1.48	33.02	62.21	259.3	149
PU REF	47	6.61	6.30	3.27	16.21	66.80	254.9	156

^aDetermined by a) Rheometer-DMTA, b) DSC and c) TGA.

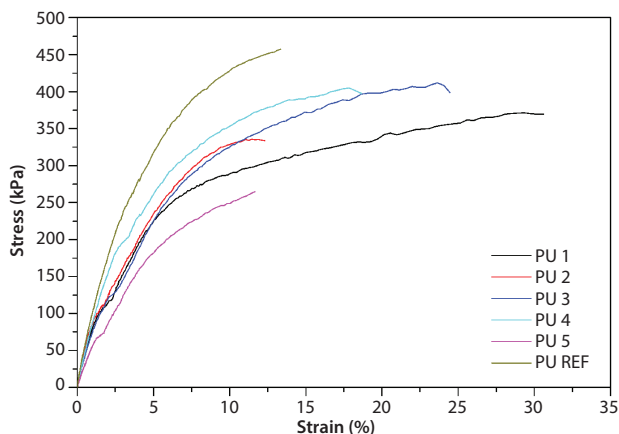


Figure 3 Tensile stress-strain curves for biobased PU foams.

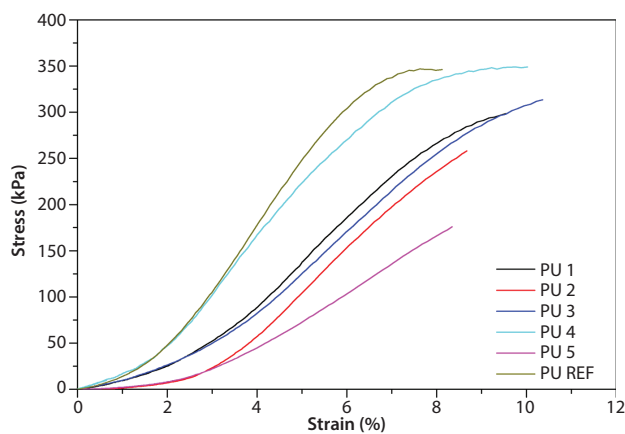


Figure 4 Compressive stress-strain curves for biobased PU foams.

PU REF presents the higher Young's modulus but not the higher elongation at break; that happens because PU REF behaves as a fragile material. Three of the biobased PU samples have similar Young's modulus values where the main difference between these curves is the elongation at breaking point; PU 1 and PU 3 have the higher values with 31% and 25% respectively.

As a result, PU foams with higher content of diols would resist higher values of strain because of the presence of hydrogen bonds produced by the presence of short diols (Figure 1a). Also, the higher molecular weight of the linear macrodiol can be translated into longer polymer chains, so increasing the macrodiol content produced a good distribution of the load throughout the polymer network [25].

As was predicted, the lowest quality foams in compression mode (Figure 4) were obtained with the high content of macrotriol samples due to the high content of macrotriol in the prepolymer formulation. This

implies a softer final material than commercial polyester polyol foams due to branched chains that do not allow good packaging of polymer chains. Moreover, mechanical properties of the final PU foams are affected by the kind of polyol used in the synthesis. They can be prepared prepolymers with lineal long chains, combining biobased polyol aromatic structure polyols in the PU polymer matrix that allow good packaging of polymer chains [19], resulting in a similar performance material in comparison with commercial petro-based PU foams on the national market.

In general, PU 4 has better mechanical properties than other bio-foams; the PU 4 sample presents the nearest mechanical behavior with respect to PU REF. It is possible to explain this fact due to the higher content of short chain diol that gives the final polymer backbone a higher frequency of urethane groups, interacting with hydrogen bonds between polymer chains and giving strength to the foam.

3.3 Thermal Properties of Foams

3.3.1 Differential Scanning Calorimetry

The curing temperature, T_c and glass transition temperature, T_g , of foams can be determined with DSC curves. There is a relation between these properties and the reactivity of the polyols. In spite of branched macrotriols being less reactive than short chain diols and macrodiols due to steric hindrance of the molecules [26], a higher macrotriol content in the prepolymer reduces the hydrogen bond interactions between chains (Figure 1 at the N-H interactions zone). This gives the molecules more mobility and increases the possibility of OH groups reacting, the result of which is a foam that would require less temperature to be cured completely. Besides, increasing the short chain diol content, which is highly reactive because of the molecule size, also decreases the T_c .

The T_c temperature is associated with a temperature at which chains are moving and reacting with functional groups, so long chains will require more energy (or more temperature) to start moving. PU 3 and PU 4 have the lowest T_c value because of the presence of short diol molecules, so they have more mobility. PU 5 has the lowest T_c value because the high content of long hydrocarbon chains in the macrotriol gives the molecules more flexibility, so they can move with more facility [27]. On the other hand, PU 1 has the highest T_c because of the presence of the highest content of macrodiol.

The T_g values are reported in Table 3, where greater differences are seen between the PU 5 ($T_g = 33.02$ °C) and the other bio-foams due to increasing macrotriol content; higher T_g is achieved because the macrotriol

causes a high crosslinking density in the polymer matrix. On the other hand, foams with higher content of linear diols cause lower T_g values [28]. This fact is attributed to the rigidity of the polymer network because short chain diols are able to create more hydrogen bonding between polymer chains, so a polymer chain with higher frequency of urethane groups (hard segment of chains) is obtained [26, 28].

3.3.2 Thermogravimetric Analysis

The thermal stability of the biobased PUs was studied by TGA and the $T_{10\%}$ values (temperature at which the sample has lost 10% of the initial weight) are shown in Table 3. As expected, thermal stability presents similar behavior between the commercial foam and biobased foams, presenting a single-step drop at the typical degradation temperature of urethane bonds (around 250–255 °C) [29]. In spite of the presence of a single-step drop, there are two peaks in the derivate curve ($\%/^{\circ}\text{C}$) due to a change of the curve slope when it is descending; the first peak corresponds to the decomposition of urethane groups (related to hard segments of the chain) and then the decomposition process is followed by another peak which is attributed to C-C, correlated with the soft-segment concentration and suggesting that degradation starts in the hard segment [30]. Figure 5 shows this change in the % weight vs. temperature derivate curve.

Higher $T_{10\%}$ values of this temperature were observed in foams with the addition of macrotriol. This happens because of the presence of trifunctional polyols that help chains to crosslink better into the polymer matrix, resulting in a more rigid network that requires more temperature to break the polymer chains; as shown in Figure 5, PU hard segments start to degrade at higher temperatures than soft segments [31]. The best result for the thermal stability was obtained by PU 5 with 259.3 °C for $T_{10\%}$ temperature, but it can be concluded that biobased PU foams have a similar behavior with respect to PU REF, based on conventional polyols.

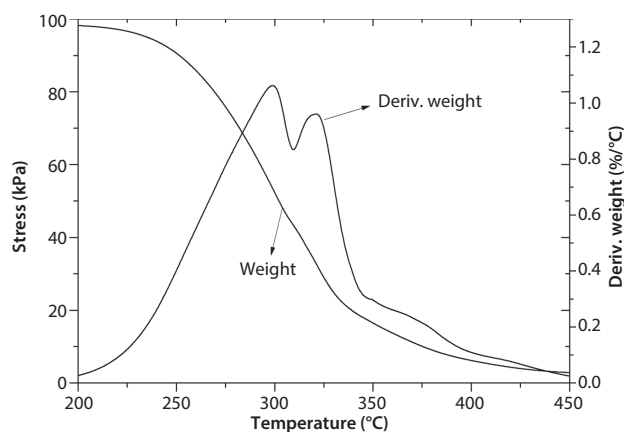


Figure 5 Weight vs. temperature derivate curve of PU foams.

3.4 Dynamic Mechanical Thermal Analysis of Foams

$\tan \delta$ temperature ($T_{\tan \delta}$) can be determined through DMTA curves, where oscillatory stress was applied to PU foams. In this case, stresses are used that cause 0.2% of strain in torsion with a 3 °C/min ramp temperature from 25 °C to 250 °C. Figure 6 shows the dependence of $\tan \delta$ on changing the bio-polyol content in the prepolymer. This property ($T_{\tan \delta}$) is strongly linked with the structure formed into the foam's network after the isocyanate-polyol reaction.

As shown in Figure 6, PU 1 curve (foam with the lowest content of macrotriol in the prepolymer) presents the higher $\tan \delta$ peak. As the crosslink density increases, the rubber transition becomes less pronounced [32] and the height of the $\tan \delta$ peak decreases, so the highest $\tan \delta$ value of PU 1 specifies that this foam has a lower crosslink density. This fact could be expected according to Table 1, which indicates that PU 1 has the lowest content of macrotriol (polyol associated with the crosslinking effect). The presence of diols produces only lineal chains.

In this case, PU 5 has the higher $T_{\tan \delta}$ of all families, because when macrotriol content is increased in prepolymers, freedom of segmental mobility of the polymer chain is restricted and highly crosslinked polymer networks are produced, so the chain requires a higher temperature to allow the polymer chains to start flowing. Also, $T_{\tan \delta}$ depends linearly on the molecular weight of chains, which can be explained by a free volume argument [33]. Higher content of macrodiol (higher molecular weight than short chain diol) results in more flexible chain, therefore lower $T_{\tan \delta}$. It is important to consider that long lineal chains could get tangled with other lineal chains, causing less mobility in the polymeric matrix; but according to $\nu_{\text{Free N-H}}$ stretching peak of the FTIR spectrums, PU 1 presents

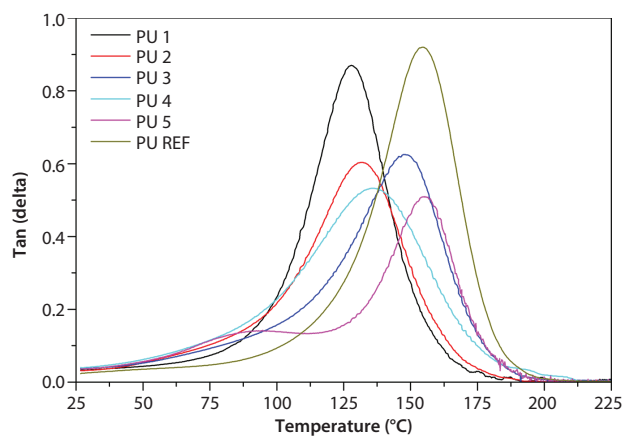


Figure 6 $\tan \delta$ behavior for different biobased PUs.

the higher content of free N-H groups. That means less intermolecular interactions between chains. For this reason, the PU 1 sample has the lowest $T_{\tan\delta}$.

According to the results shown in Figure 6, we can conclude that PU 5 foam has the most crosslinked network, presenting a very similar $T_{\tan\delta}$ value compared to PU REF (149 °C and 156 °C, respectively); a result that is also associated with the difficult movement of the polymer chains.

Storage modulus (G') curves of the PU foams are shown in Figure 7. The curves are obtained by DMTA testing, measuring the behavior of foams to a cyclic deformation as a function of temperature. The polymeric matrix consists of chemical crosslinks and physical crosslinks, including entanglements, loose chain ends and lattice interaction in crystalline domains [5], so storage modulus curves are strongly related to this crosslink density.

According to Figure 7, the initial G' values (rubbery plateau modulus) were higher for PU with higher content of macrodiol, and presented the lowest rubbery plateau modulus for those samples with higher content of macrotriol. This is consistent with the highest functionality of macrotriol, producing more chemical crosslinks. Samples with higher crosslink density impede movement more than samples with higher content of diols [4], independent of their molecular weight.

Differences between PU 2, PU 3 and P4 are attributed to the content of short chain diol. The function of diols is mainly to extend the polymer chains (produce higher molecular weight of chains) with the modification of the frequency of the urethane groups. Increasing the urethane groups' frequency along the chain (hard segments) promotes interactions with other polymer chains by H-bonding and decreases

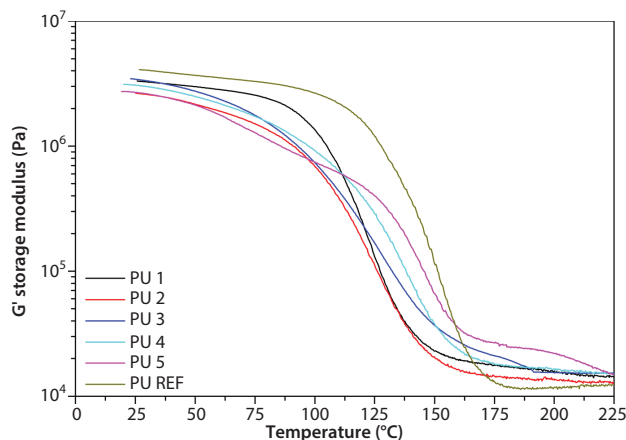


Figure 7 Storage modulus vs. temperature behavior for different biobased PUs.

the free movement of the matrix. In spite of the lower intensity at $\sim 1528\text{ cm}^{-1}$ peak (Figure 2), a signal attributed to the N-H bending of the urethane groups, physical crosslinking between chains can increase with the higher short chain diol content, and because of that, presents lower rubbery plateau modulus values than PU 1. Figure 1a shows the variation of the 3500 cm^{-1} peak intensity, corresponding to the non-H-bonded one.

All the samples with the exception of PU 5 show one thermal transition related to a thermal transition of the hard segments. Sample with 100% of macrotriol exhibited two thermal transitions, as shown in Figure 7, probably due to a crystallization of long aliphatic chains in the matrix [34]. The higher drops of G' are for PU 1 sample due to the movement of chains at high temperatures. These chains are bigger and more flexible than chains with higher macrotriol content. The PU REF sample exhibits the highest rubbery plateau modulus that would be produced by a restriction of movement for the polymer chains. This fact can be confirmed according to Figure 1a; the 3500 cm^{-1} peak corresponding to the non-H-bonded N-H group, shows the lowest intensity for the PU REF sample and the 1060 cm^{-1} peak associated with C-O bonds of urethane groups exhibits the absence of another little peak at higher wavenumber in this zone, related to the non-bound C-O groups by H-bond interactions. In conclusion, PU REF chains have the lowest mobility because of the intermolecular interactions with other polymer chains.

3.5 Shape Memory

Figure 8 shows the stress-strain-temperature relation of biobased PU foams up to 3 kPa stress. As expected, the stress increases with strain, according to Figure 2, which shows the stress-strain curves in torsion mode. The residual strain increases with the macrotriol content, a fact caused by internal molecular rearrangement and chain disentanglements that could happen with less facility than those in foams with higher content of short chain diol [35].

Netpoints are responsible for determining the permanent shape of the polymer network and can be of a chemical (covalent bonds) or physical (intermolecular interactions) nature. However, if a chemical reaction occurs in the material at high temperatures, new bonds can be formed, resulting in loss of shape memory of the polymer for both physical and chemical crosslinks [36]. Physical crosslinks are obtained by vitrification or crystallization of many chains at $T_{\tan\delta}$ by attaching functional groups to chain segments.

According to Figure 8, PU 5 sample was incapable of fixing strain; that is, the strain diminished from

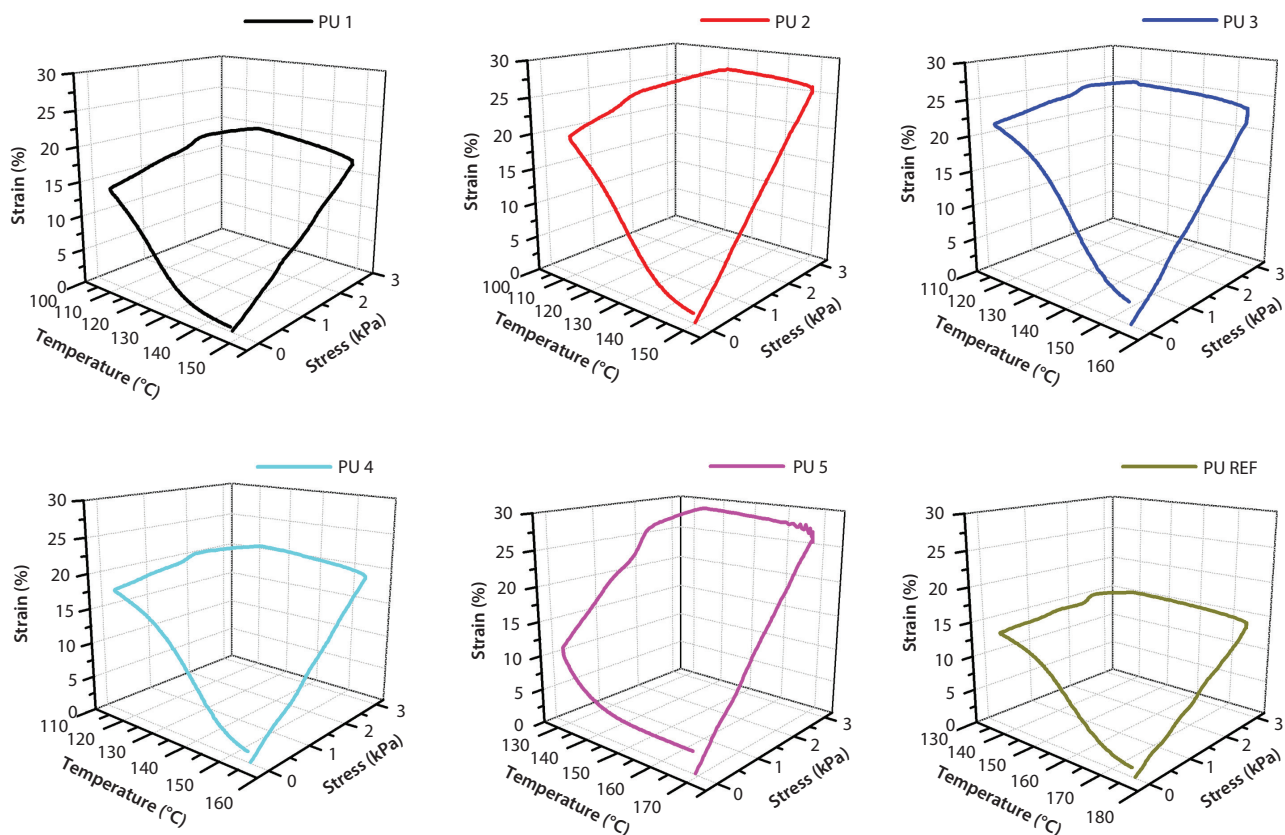


Figure 8 Shape memory curves for biobased PU foams.

28% to almost 9% when the stress was released, representing a 41% shape fixity value for this sample. That happens because macrotriol produces flexibility in the matrix and after applying the strain, new interactions between molecules are not as good as other samples. In contrast, after increasing the short chain diol, PU 3 and PU 4 presented 88.5% and 85.8% shape fixity values that can be compared with the commercial sample (89.9%). When the sample is deformed, chains move to create new intermolecular forces in the polymer matrix, so chains with high frequency of hard segments would produce more new interactions than samples with more content of soft segments; the C=O group of the hard segments explains this fact because of the creation of new H-bonds.

In Table 4, it is seen that the shape fixity decreases with increasing high molecular weight polyol content and functionality of the polyol. According to Figure 7, there is a relation between rubbery plateau modulus and shape fixity [18] and 2,4/2,6-toluene diisocyanate (TDI-80; this is because below $T_{\tan\delta}$ the material acts in the rubbery plateau modulus range. Nevertheless, a pattern between shape recovery and rubbery flow modulus is not shown.

Table 4 Shape fixity and shape recovery values of PU rigid foams.

Sample	Shape fixity (%)	Shape Recovery (%)
PU 1	75.4	96.7
PU 2	74.5	95.1
PU 3	88.5	87.4
PU 4	85.8	93.0
PU 5	41.0	89.1
PU REF	89.9	91.7

Biobased polyurethanes showed good shape recovery, although PU 5 showed the worst shape recovery. This could be attributed to the presence of more physical crosslinking in the other samples due to the highest frequency of urethane bonds, which caused the storage of more deformed energy in the system [9]. Samples with lower $T_{\tan\delta}$ values (Table 3) showed higher shape recovery. This could be explained because of the restricted mobility of long chains and highly crosslinked polymer networks. High mobility of chains would produce the recovery

of the initial state when the stress is released; but also below $T_{\tan \delta}$, new weak interactions forming (mainly van der Waals forces) between chains cannot fix their position, allowing the chains to move when they are heated. According to Figure 1, PU 1 and PU 2 present the higher content of free N-H groups. For this reason, these samples have the highest shape recovery percentages.

4 CONCLUSIONS

High content of macrotriol in the prepolymer formulation implies a softer final material. PU 4 with the higher content of short chain diol has better mechanical properties obtaining a 5.58 MPa elastic modulus in compression compared with 6.61 MPa obtained from commercial foam.

There are no considerable differences in degradation temperatures between synthesized biobased PU foams. At 10% of lost weight, all degradation temperatures are between 250 °C and 256 °C.

Due to the higher crosslinked polymer network and the absence of short chain diol and macrodiol, PU 5 has the highest $T_{\tan \delta}$ of all biobased prepolymer families. The $T_{\tan \delta}$ obtained in this PU family is 149, close to that of 156 °C found in commercial foam.

Increasing the short chain diol content in the prepolymer would produce higher frequency of urethane groups in polymer chains, able to interact and create physical crosslinks with other chains. This translates into higher shape fixity values.

ACKNOWLEDGMENTS

The authors wish to thank GOVAN PROJECTS S.A. for financial support during this study and National Laboratory of Nanotechnology (LANOTEC) for all the facilities provided during the material characterization process.

REFERENCES

1. T. Gurunathan, S. Mohanty, and S.K. Nayak, Isocyanate terminated castor oil-based polyurethane prepolymer: Synthesis and characterization. *Prog. Org. Coatings* **80**, 39–48 (2015).
2. E. Sharmin and F. Zafar, Polyurethane: An introduction, in *Polyurethane*, pp. 3–16, InTech (2012).
3. K. Khemani, Polymeric foams: An overview, in *Polymeric Foams: Science and Technology*, ACS Symposium Series, American Chemical Society, Washington DC, USA (1997).
4. Z. Petrovic, Polyurethanes from vegetable oils. *Polym. Rev.* **48**(1), 109–155 (2008).
5. H. Yeganeh and P. Hojati-Talemi, Preparation and properties of novel biodegradable polyurethane networks based on castor oil and poly(ethylene glycol). *Polym. Degrad. Stab.* **92**(3), 480–489 (2007).
6. D.V. Palaskar, A. Boyer, E. Cloutet, C. Alfos, and H. Cramail, Synthesis of biobased polyurethane from oleic and ricinoleic acids as the renewable resources via the AB-type self-condensation approach. *Biomacromolecules* **11**(5), 1202–1211 (2010).
7. T. Garrison and M. Kessler, Plant oil-based polyurethanes, in *Bio-based Plant Oil Polymers and Composites*, pp. 37–54, Elsevier Inc., UK (2016).
8. G.T. Howard, Biodegradation of polyurethane: A review. *Int. Biodeterior. Biodegrad.* **49**(4), 245–252 (2002).
9. H. Kalita and N. Karak, Biobased hyperbranched shape-memory polyurethanes: Effect of different vegetable oils. *J. Appl. Polym. Sci.* **131**(1), 1–8 (2014).
10. S. Miao, P. Wang, Z. Su, and S. Zhang, Vegetable-oil-based polymers as future polymeric biomaterials. *Acta Biomater.* **10**(4), 1692–1704 (2014).
11. M. Zhang and Y. Yu, Dehydration of ethanol to ethylene. *Ind. Eng. Chem. Res.* **52**(28), 9505–9514 (2013).
12. D. Fan, D.J. Dai, and H.S. Wu, Ethylene formation by catalytic dehydration of ethanol with industrial considerations. *Materials (Basel)* **6**(1), 101–115 (2013).
13. Y. Cao, J. Wang, Q. Li, N. Yin, Z. Liu, M. Kang, and Y. Zhu, Hydrolytic hydrogenation of cellulose over Ni-WO₃/SBA-15 catalysts. *J. Fuel Chem. Technol.* **41**(8), 943–949 (2013).
14. Y. Cao, J. Wang, M. Kang, and Y. Zhu, Efficient synthesis of ethylene glycol from cellulose over Ni-WO₃/SBA-15 catalysts. *J. Mol. Catal. A Chem.* **381**, 46–53 (2014).
15. Standard test method for isocyanate groups in urethane materials or prepolymers, ASTM D2572 – 97 (2010).
16. Standard test method for acid value of fatty acids and polymerized fatty acids, ASTM D1980 – 87 (1998).
17. Standard test methods for testing polyurethane raw materials: Determination of hydroxyl numbers of polyols, ASTM D4274 – 16 (2016).
18. S.M. Kang, S.J. Lee, and B.K. Kim, Shape memory polyurethane foams. *Express Polym. Lett.* **6**(1), 63–69 (2012).
19. M. Kirpluks, U. Cabulis, A. Ivdre, M. Kuranska, M. Zieleniewska, and M. Auguscik, Mechanical and thermal properties of high-density rigid polyurethane foams from renewable resources. *J. Renew. Mater.* **4**(1), 86–100 (2016).
20. M. Coleman, K. Lee, D. Skrovanek, and P. Painter, Hydrogen bonding in polymers. 4. Infrared temperature studies of a simple polyurethane. *Macromolecules* **19**(8), 2149–2157 (1986).
21. C. Lluch, B. Esteve-Zarzoso, A. Bordons, G. Lligadas, J.C. Ronda, M. Galia, and V. Cádiz, Antimicrobial polyurethane thermosets based on undecylenic acid: Synthesis and evaluation. *Macromol. Biosci.* **14**(8), 1170–1180 (2014).
22. Y. Tao, A. Hasan, G. Deeb, C. Hu, and H. Han, Rheological and mechanical behavior of silk fibroin reinforced waterborne polyurethane. *Polymers (Basel)* **8**(3), 94 (2016).
23. M. Włoch and J. Datta, Synthesis, structure and properties of poly(ester-urethane-urea)s synthesized using biobased diamine. *J. Renew. Mater.* **4**(1), 72–77 (2016).

24. K. Gorna, S. Polowinski, and S. Gogolewski, Synthesis and characterization of biodegradable poly(ϵ -caprolactone urethane)s. I. Effect of the polyol molecular weight, catalyst, and chain extender on the molecular and physical characteristics. *J. Polym. Sci. Part A Polym. Chem.* **40**(1), 156–170 (2002).
25. S. Oprea, Effect of the long chain extender on the properties of linear and castor oil cross-linked PEG-based polyurethane elastomers. *J. Mater. Sci.* **46**(7), 2251–2258 (2011).
26. R. Gu, S. Konar, and M. Sain, Preparation and characterization of sustainable polyurethane foams from soybean oils. *J. Am. Oil Chem. Soc.* **89**(11), 2103–2111 (2012).
27. F. Seniha Güner, Y. Yağci, and A. Tuncer Erciyes, Polymers from triglyceride oils. *Prog. Polym. Sci.* **31**(7), 633–670 (2006).
28. H. Bunjes, K. Westesen, and M.H.J. Koch, Crystallization tendency and polymorphic transitions in triglyceride nanoparticles. *Int. J. Pharm.* **129**(1–2), 159–173 (1996).
29. J. Chambers, J. Jiricny, and C.B. Reese, The thermal decomposition of polyurethanes and polyisocyanurates. *Fire Mater.* **5**(4), 133–141 (1981).
30. Z.S. Petrovic, Z. Zavargo, J.H. Flynn, and W.J. Macknight, Thermal-degradation of segmented polyurethanes. *J. Appl. Polym. Sci.* **51**(6), 1087–1095 (1994).
31. A. Wolska, M. Goździkiewicz, and J. Ryszkowska, Thermal and mechanical behaviour of flexible polyurethane foams modified with graphite and phosphorous fillers. *J. Mater. Sci.* **47**(15), 5627–5634 (2012).
32. H. Lim, S.H. Kim, and B.K. Kim, Effects of the hydroxyl value of polyol in rigid polyurethane foams. *Polym. Adv. Technol.* **19**(12), 1729–1734 (2008).
33. L. Wu, J. Van Gemert, and R.E. Camargo, *Rheology Study in Polyurethane Rigid Foams*, Huntsman Corp., Michigan, United States (2012).
34. V. Pistor, D. De Conto, F.G. Ornaghi, and A.J. Zattera, Microstructure and crystallization kinetics of polyurethane thermoplastics containing trisilanol isobutyl POSS. *J. Nanomater.* **2012**, 283031 (2012).
35. M. Ahmad, B. Xu, H. Purnawali, Y. Fu, W. Huang, M. MirafTAB, and J. Luo, High performance shape memory polyurethane synthesized with high molecular weight polyol as the soft segment. *Appl. Sci.* **2**(2), 535–548 (2012).
36. P. Singhal, J. Rodríguez, W. Small, S. Eagleston, J. Van De Water, D. Maitland, and T.S. Wilson, Ultra low density and highly crosslinked biocompatible shape memory polyurethane foams. *J. Polym. Sci. Polym. Phys.* **50**(10), 724–737 (2012).